Effect of Directivity in Northeastern ALBANIA (5.4 M_W) Earthquake of September 6, 2009, from Radiated Seismic Energy

Edmond Dushi[1], Rrapo Ormeni[2]

[1,2]*Department of Seismology, Institute of Geosciences, Energy, Water and Environment, Polytechnic University of Tirana, Albania.*

ABSTRACT

We have quantitatively estimated an observed directivity effect, direct from the radiated seismic energy of September 6, 2009, in north-eastern Albania. Despite its moderate magnitude (Mw = 5.4), much damage was caused from this earthquake in its epicenter area, being broadly felt. Field observations, in near field to the causative fault, demonstrated a directional shaking effect pronounced mostly westward with severe effects at Çereneci and Shupenza localities.

Earthquake has been instrumentally recorded from ASN and several regional broadband seismic stations, being thus the strongest event occurred since 2007, within Albanian territory. We estimated the radiated seismic energy from corrected broadband waveforms. It is considered as the most important parameter relating the dynamics and the observed directivity effect of the causative fault. A finite source model is considered, though in its simplified form it was assumed as a point source, an approximation used throughout the spectral analysis.

Based on energy we could estimate the effect of directivity varying within the interval 0.0004 - 6.0, as an absolute factor on cumulative spectrum at different azimuthal angles on the focal sphere. Results are in accordance with fault geometry determined from focal mechanism solution. Earthquake of September 6, 2009 was caused from a normal fault system, striking 220^0, dipping 40^0 and slipping -90^0.

The effect of directivity on radiated energy, in far field was more pronounced at TIR and PUK stations and less detected at PHP and BCI stations, nearly at the opposite of the active fault striking direction.

INTRODUCTION

On September 6, 2009 at 21:49 (UTC), an earthquake of $M_W = 5.4$ occurred about19 *km* southern of Peshkopia in northeastern Albania, within the Dibra district [1]. Its hypocenter was localized in the vicinity of Gjorica village causing severe damage in the epicenter area. The shake has been strongly felt in almost interely Dibra district, but also in Burreli, Tirana, Librazhdi and Elbasani. From field observations, evidences about relief cracks, dueling houses damages or partially and completely destroyed buildings, were documented [2]. These data are used to interpret and explain the geological and tectonic conditions that triggered this event. It resulted the strongest event occurred in NE extremity of Vlora-Elbasani-Dibra transverse fault zone (VED), after that of November 30, 1967, despite its moderate energy released. Occurence of this event asigned a peak in the long seismic activity, released along VED, since 2004.

The event of September 6, is recorded from six broadband seismic stations belonging to ASN, and also by neighbor networks. Its main shock was imediately followed from a great number of aftershocks, some of them strong enough to be felt. The strongest aftershocks were those of September 6 at 22:01 (UTC) with $M_W = 3.8$ and September 7 at 09:48 (UTC) and 15:20 (UTC), with $M_W = 3.8$ and $M_W = 3.7$, respectively. In total 678 recorded events, from which 130 localizable, were registered into the national database [1].

Based in the near field observations, effects of the earthquake's main shake, were more pronounced to the western and south-western regions of the affected area. In the far field, high energy values are achieved for recordings of TIR and PUK, at $AZM = 251^0$ and $AZM = 318^0$, respectively. Above azimuthal directions coincide with the stress field orientation from the achived focal mechanism solution. Less energy results at PHP and BCI stations, due to their position in the antipode of the strike direction $AZM = 210^0$. These results, together with the visual analysis of waveforms and displacement spectra, suggests a directivity effect on radiated seismic energy from a normal fault system that triggered the September 6, 2009 earthquake.

We computet seismic energy, from corrected waveform traces in six broadband stations, which we think is the most important macroscopic parameter relating the dynamics of the activated fault segment with the observed directivity effect. This procedure has been broadly known [3]. Our intention has been to support observed macroseismic effects with a clear instrumental base as well as the focal mechanism solution achived for this earthquake. All steps of computation and the method used are discussed throughout this paper.

INSTRUMENTAL DATA USED AND THEIR COMPUTATION

Analysis presented herein is based on instrumental recorded data for the main shock and major subsequent aftershocks, (Tab. 1). Prior to spectral analysis, waveforms are corrected and conditioned, in order to be appropriate for further elaboration. These data consist of broadband seismological signals, recorded in a range from 0.03 Hz up to 30 Hz and sampled at 100 sps.

These records were contribution of six operational stations of ASN respectively: BCI, PHP, PUK, TIR, KBN and SRN, shown in figure 1.

Waveforms are processed with *Mulplt* software routine in *Seisan ver. 9.1*, [4]. Only secondary S_g /S_n body waves has been used, which are dominant and well recorded in longitudinal (N-S) and transversal (E-W) components. By mean of band-pass filters in the frequency band 1.0 - 6.0 Hz, higher SNR values are achieved, to determine and correctly select this wave group. Because of being of Butterworth type, these filters introduce a flat response in the selected frequency interval, to the recorded signal. Also other different frequency intervals were tried for comparative results.

S-waves are chosen as appropriate because they contain more than *95 %* of radiated seismic energy radiated out of a seismic source. They are also dominant at local and regional distance, thus scattered energy within its coda part can be well detected and excluded from further computations.

Selected wave groups, for each recording component and seismic station, are plotted in figure 1. A set of 15 wave groups are selected, for which a direct visual analyze is done, after smoothing with a three-point averaging procedure. Plotted waveforms are displacement records with amplitudes in *nm*. They were corrected for system response.
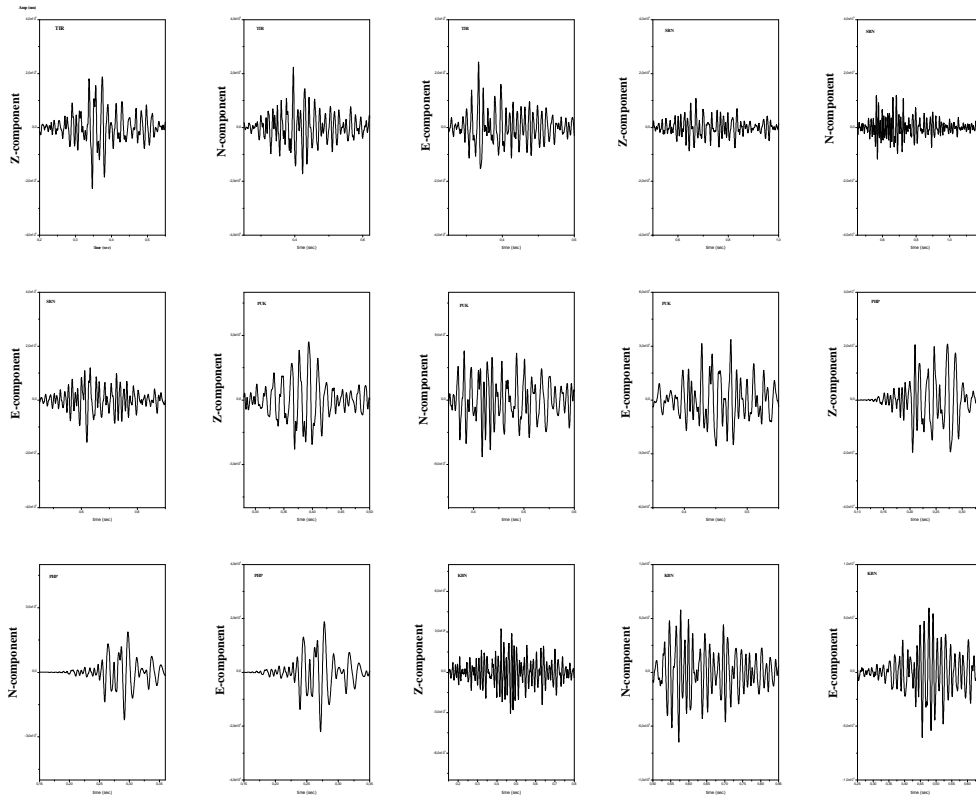
Figure 1 Selected S wave groups for the September 6, 2009 earthquake.

Correction of waveform data

Spectral corrections are carried out prior of evaluating the source parameters and radiated seismic energy. After correcting for instrument response, displacement spectra accounting for finite spectral source function were achieved, despite broadband records. This process is done using *Mulplt* routine in *Seisan* package [4]. Response information of ASN system was arranged appropriately as the input to compute the discrete correction coefficients in frequency domain.

Path effect comprises a contribution of both geometrical spreading and attenuation due to mean absorption and scattering of wave energy. Considering the geometrical spreading as inverse function of the distance, as established by Herman and Kijko (1983) and adopted in *Seisan* , equation (1) and (2) are used for epicenter distances less and greater than 100 *km* and depths less than 50 *km*, respectively.

$$G(\Delta, h) = GD^{-\beta} = \left(\Delta^2 + h^2\right)^{-\frac{\beta}{2}} \tag{1}$$

$$G(\Delta, h) = GD^{-\beta} = \left(\Delta \cdot \Delta_0\right)^{-\frac{\beta}{2}} \tag{2}$$

In equations (1) and (2), *GD* is termed *geo-distance*; Δ *(km)* is the epicenter distance; Δ_0 *(km)* is the reference distance named as *Herkij-distance* equals 100 *km*; *h (km)* is the hypocenter depth and β is the wave-dependent parameter. Secondary body waves S (S_g/S_n) have a β = 1.0, [5]. Geo-distance term differs respectively between (1) to (2), relating epicenter distance and event depth.

Attenuation, caused at discontinuities and lateral heterogeneities, is very important in seismic energy computation. To correct for these effect, we have developed a local quality model function *Q (f)* applying the well-known single back-scattering method on S-coda part, [6]. Effect of attenuation at the most upper surface layers, expressed as the high frequency diminution parameter κ, is determined and integrated within this model. Thus, September 6, 2009 wave-traces were corrected for mean attenuation effect, using the model (3).

$$A(f,t) = e^{-\pi f \kappa} \cdot e^{\frac{-\pi ft}{Q(f)}} = e^{-\pi f(0.05)} \cdot e^{\frac{-\pi ft}{(84) f^{0.84}}} \qquad (3)$$

In equation (3), = 0.05 express the mean diminution parameter; $Q_0 = 84$ express the quality factor value at $f = 1$ Hz and = 0.84 is the frequency dependent parameter.

To correct for the radiation pattern effect only, the parameter R , = 0.63 is applied in the spectral model used to process data. Applying correction for radiation pattern, a back-projection of all independent traces on the focal sphere is achieved, assuming the source as a point source despite its finite length. Thus, we suggest that correcting as above only the effect of directivity would influenced the spectral amplitudes, leading to a non-uniform distribution of radiated seismic energy.

Seismic Energy

Seismic energy is determined through integration of square velocity spectra, as the sum of discrete quadratic velocity values, in frequency domain [7]. Applying FFT analysis, velocity spectra were obtained from displacement, multiplying by = 2 f.

Through this method, single station energy estimation $E_{i,j}$ ($i, j = 1...N$) is obtained at different azimuth angles j from the fault's strike direction i. Equation (4) is used to integrate in frequency domain.

$$E_{S i,j} = (4\pi R^2) \cdot \rho \upsilon \cdot \sum_{f=1}^{N} (V_{i,j})^2 (N \cdot \Delta t^{-1}) \qquad (4)$$

In equation (4), R express the slant distance; ($N \cdot$ t^{-1}) factor is the sampling interval f depending on the number of samples and sampling rate. Radiated source energy is obtained thus as cumulative energy spectrum. Applying *Brune* model, we computed along with the energy also the main source parameters, which are listed in table 1.

Uniting the radiated energy estimated at each station into an integral estimation we account for the variation of the energy over the focal sphere. For a line source, which is the case under study with strike angle i, defined from focal mechanism solution, and the takeoff angle for any ray between the source and station j is j, the radiated energy $E_{i,j}$ depends on (i - j) only without considering the directivity effect, [8]. Thus, we used expression (5) which calculates the average over stations, taking into account the above described fault model.

Date	Time	Lat.	Lon.	Dep.	M_w	f_0		$_0$	a	M_0	E_s
mm/dd	*hh:mm*	*N-S*	*E-W*	*km*		*sec*	*bar*	*mHz^{-1}*	*km*	*dyn/cm*	*erg*

$$\overline{E_i} = \sum_{j}^{N} w_j E_{i,j} / \sum_{j}^{N} w_j \tag{5}$$

In equation (5), $w_j = [1 - \cos(_i - _j)]$. Results obtained are listed in table 1, in the following, while cumulative energy and displacement spectra are plotted in figure 2.

09/06	21:49	41.51	20.46	15	5.2	0.6	24	1.0E-3	2.2	6.0E+23	1.9E+20
09/06	22:01	41.48	20.47	16	3.8	1.9	7.6	1.0E-4	0.7	6.0E+21	2.8E+19
09/06	22:24	41.52	20.51	15	3.5	3.7	28.1	2.0E-5	0.4	3.0E+21	2.3E+18
09/06	22:36	41.43	20.43	7	3.3	3.4	7.3	4.0E-6	0.4	1.0E+21	1.8E+17
09/06	23:31	41.53	20.46	6	3.2	2.5	2.3	6.0E-6	0.5	8.0E+20	2.7E+17
09/07	00:11	41.49	20.46	15	3.4	4.2	27.4	1.0E-5	0.3	2.0E+21	3.4E+18
09/07	03:52	41.46	20.52	15	3.1	3.0	2.5	3.0E-6	0.4	5.0E+20	6.5E+15
09/07	04:03	41.41	20.51	20	3.1	2.8	2.0	3.0E-6	0.5	5.0E+20	3.9E+16
09/07	04:22	41.41	20.51	17	3.2	1.0	0.1	4.0E-6	1.3	8.0E+20	3.7E+16
09/07	09:48	41.44	20.44	13	3.8	0.9	0.8	5.0E-5	1.5	6.0E+21	4.8E+17
09/07	12:21	41.42	20.41	12	3.3	1.2	0.3	3.0E-6	1.1	1.0E+21	1.3E+16
09/07	13:04	41.45	20.44	10	3.0	1.5	0.2	1.0E-6	0.9	4.0E+20	2.6E+16
09/07	13:42	41.44	20.46	20	3.4	1.1	0.2	4.0E-6	1.2	1.0E+21	1.2E+16
09/07	14:19	41.44	20.46	15	3.4	1.1	0.2	5.0E-6	1.2	1.0E+21	1.9E+16
09/07	15:20	41.46	20.46	15	3.7	1.2	1.3	1.0E-5	1.1	4.0E+21	1.0E+17

Table 1 Source parameters from spectral analyze of the September 6, 2009 main shock (M_W 5.4) and its subsequent aftershocks (M > 3.0).
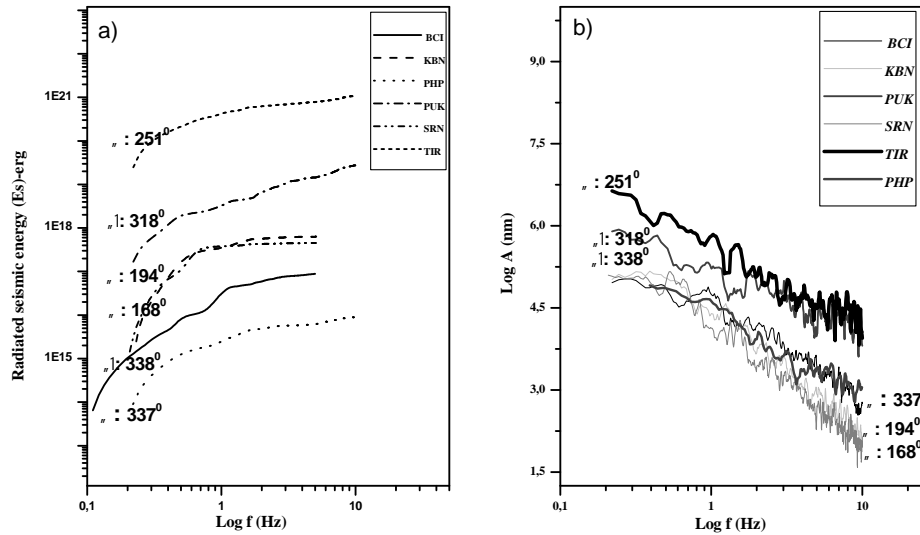
Figure 2 seismic energy (a) and displacement source spectra (b) at different azimuths on the focal sphere.

Focal Mechanism Solution

Focal mechanism solution is computed using *Focmec* program, integrated in *Seisan*, [9]. To attempt a solution, we used polarities of first onsets of primary body waves, and the amplitudes of P-waves and S-waves, to refine the solution. Amplitudes are picked on P-wave trains, in vertical components, and S-wave groups in longitudinal and transversal ones.

Solution is based in the location accuracy. Thus, first we have performed the event location applying the method of trial depth by fixing it at 10 km. The first solution was located 15 km from the nearest station PHP. Through an iterative procedure, the errors are minimized, to increase the resolution. The program used is *Hypocenter v. 3.2*, [10].
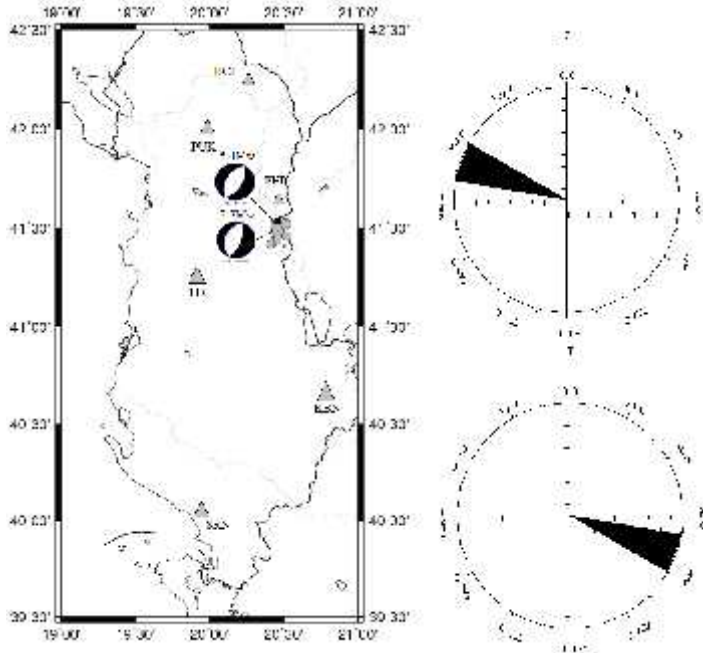
Figure 3 Focal mechanism solutions, for main shock and its immediate aftershock, and the azimuthal distribution of principal strain axis (P, T), corresponding to direction of stress field distribution.

Results obtained define a normal fault system striking 210^0 SSW, with an active plane dipping almost 40^0 to the east and slipping – 90^0, as the causative fault for the event of September 6, 2009 (M_W 5.4). Parameters determined for the double couple model define an auxiliary plane striking 30^0, dipping 40^0 to the west and dipping – 90^0. The achieved solution for the main event and the immediate subsequent aftershock at 22:01 (UTC), are plotted in the map of figure 3.

Strike and dip angles for the principal strain axes, which values are plotted as polar diagrams in figure 3, show a main direction of the dilatational movement (P-axes) striking 300^0 to the WNW and dipping 85^0, while the compressional movement (T-axes) strikes 120^0 ESE and dips 5^0. Results are consistent with field macro-seismic observations.

DIRECTIVITY ANALYSIS
Directivity effect is explicit in displacement spectra (figure 2), after comparing modeled source function at different angles from strike direction. Spectral level is then given as a decade log of displacement amplitudes varying with frequency. Values of zero frequency spectral level $_0$ (*nm*) are plotted in a polar diagram in figure 4, corresponding to each of the stations. From this diagram, an azimuthal variation in amplitudes respect to station position is obvious, thus introducing the effect of directivity which has influenced the radiation of seismic energy out of this source. Amplitudes Spectral level, as maxima values in log scale, are estimated: 6.6 nm for

TIR station at azimuth of 251^0, in a distance of 59 km from the source; 5.8 nm for PUK station at azimuth 318^0, in a distance of nearly 80 km from the source, which are located westward of the source region; they equal 5.1nm and 5.0 nm, respectively for BCI and KBN seismic stations, located 338^0 and 168^0 eastward of source region at nearly the same distance (~ 100 km). While lower values are determined for SRN and PHP stations, at 194^0 and 337^0 each, at corresponding distances of 190 km and 19 km from the source region. Position of these stations coincide in direction with that of the fault, thus receiving lower amplitudes (figure 2).

The above effect is recognized so far, as a significant modification of energy and frequency content of elastic waves, from the smooth seismic rupture propagation. Directivity could happen, in near and far field, introducing peak motion predominance towards the fault direction and minima at the opposite. [11].
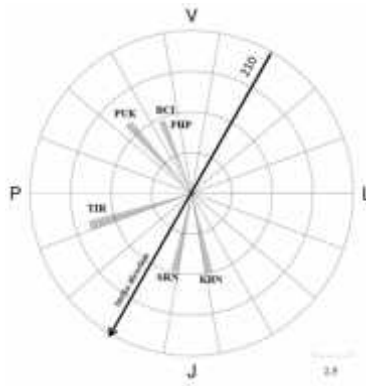

Figure 4 Diagram, plotting the polar variation of amplitude spectral level, with azimuth from the source.

We computed the effect of directivity on radiated seismic energy estimated, from the single station method (4), as described previously. Energy values achieved for each of the stations are: 8.4 x 10^{15} erg (PHP), 8.4 x 10^{16} erg (BCI), 2.75 x 10^{19} erg (PUK), 1.08 x 10^{21} erg (TIR), 6.2 x 10^{17} erg (KBN) and 4.5 x 10^{17} erg (SRN). Thus, a non-uniform distribution of seismic energy is evident. To determine the mean uniform radiated seismic energy, equation (5) is applied on this data, where $w_{i, j}$ vary from 0.05 for TIR to 1.76 for PUK. The mean radiated seismic energy corrected to achieve a homogenize distribution using (5) equals 1.9 x 10^{20} erg (Table 1). We evaluated directivity correction using the equation (6), in the following:

$$Directiv.Corr. = E_{i,j} \bigg/ \sum_{j}^{N} w_j E_{i,j} \bigg/ \sum_{j}^{N} w_j \qquad (6)$$

 Equation (6) is a result of a combination of (4) and (5), described above. Results are given in table 2, in the following.

Table 2 Directivity correction coefficients according to each recording station towards the fault orientation.

CONCLUSION

Even though the September 6, 2009 (M_W 5.4) earthquake is a moderate local event it was accompanied with directivity in the distribution of its shake effect in near field, which results also present in far field, from instrumental analysis.

Depending on the amplitude distribution and spectral shift, directivity effect has influenced the seismic energy radiation from September 6, 2009 source, due to its finite fault extension.

Despite low values of this effect, as absolute coefficients of cumulative seismic energy spectra ranging within 0.004-6.0 interval, its quantitative estimation is very important in supporting focal mechanism and field observations.

REFERENCES

[1]   Ormeni, Rr., Dushi, E., Koçi, R., (2009). The Gjorica Earthquake of September 6, 2009 (M_W = 5.4), Albania. CSEM/EMC NewsLetter No. 24, pp. 37-39.

[2]   Zaçaj, M., Dogjani, S., Dushi, E., (2009). Report on the field observations of September 6, 2009 earthquake. IGEWE archive, Tirana.

[3]   Kanamori, H. & Venkataraman, A. (2004). Effect of directivity on estimates of radiated seismic energy. *Journal of Geophysical Research*, Vol 109.

[4]   Havskov, J., Ottemöller, L, Voss, P., (2012). Seisan: earthquake analysis software v. 9.1. Department of Earth Science, University of Bergen, Norway. (manual)

[5]   Herrmann, R. B., A. Kijko (1983) Modeling some empirical vertical component Lg relations. *Bull. Seismol. Soc. Am., 73, 157–171*.

[6]   Dushi, E., (2011). Assessment of radiated seismic energy, from earthquakes in our country, using quadratic velocity spectra, PhD theses, Earth scieneces department, Geology and Mining Faculty, UPT, Tirana.

[7]   Anshu Jin and Eiichi Fukuyama (2005) Seismic Energy for Shallow Earthquakes in Southwest Japan. *Bulletin of the Seismological Society of America, Vol. 95, No. 4, pp.*

1314–1333, August 2005

[8]   Aki, K., and P. G. Richards (1980, 2002). Quantitative Seismology, W. H. Freeman, San Francisco (1980 edition). *University Science Books, Sausalito, California*

(2002edition).

[9]   Snoke, J. A., (2003). Focmec: Focal Mechanism Determinations. Virginia Tech, Blacksburg, VA, USA (http://www.geol.vt.edu/outreach/vtso/focmec).

[10]   Lienert, R. B., (1994). Hypocenter: A computer program for locating earthquakes locally, regionally and globally. Hawaii Institute of Geophysics & Planetology 2525 Correa Rd Honolulu HL (manual).

[11]   Douglas, A., Hudson, A. J., Pearce, G. R., (1988). Directivity and the Doppler effect. BSSA, Vol. 78, No. 3, pp. 1367-1372.